PLOS ONE

Fluorinated oil-surfactant mixtures with the density of water: Artificial cells for synthetic biology

Roberto Laos[1,2], Steven Benner[1]*

1 Foundation for Applied Molecular Evolution, Alachua, Florida, United States of America, 2 Panamerican Biolabs LLC, Gainesville, Florida, United States of America

* manuscripts@ffame.org

Abstract

There is a rising interest in biotechnology for the compartmentalization of biochemical reactions in water droplets. Several applications, such as the widely used digital PCR, seek to encapsulate a single molecule in a droplet to be amplified. Directed evolution, another technology with growing popularity, seeks to replicate what happens in nature by encapsulating a single gene and the protein encoded by this gene, linking genotype with phenotype. Compartmentalizing reactions in droplets also allows the experimentalist to run millions of different reactions in parallel. Compartmentalization requires a fluid that is immiscible with water and a surfactant to stabilize the droplets. While there are fluids and surfactants on the market that have been used to accomplish encapsulation, there are reported concerns with these. Span® 80, for example, a commonly used surfactant, has contaminants that interfere with various biochemical reactions. Similarly, synthetic fluids distributed by the cosmetic industry allow some researchers to produce experimental results that can be published, but then other researchers fail to reproduce some of these protocols due to the unreliable nature of these products, which are not manufactured with the intent of being used in biotechnology. The most reliable fluids, immiscible with water and suitable for biochemical reactions, are fluorinated fluids. Fluorinated compounds have the peculiar characteristic of being immiscible with water while at the same time not mixing with hydrophobic molecules. This peculiar characteristic has made fluorinated fluids attractive because it seems to be the basis of their being biologically inert. However, commercially available fluorinated fluids have densities between 1.4 to 1.6 g/mL. The higher-than-water density of fluorinated oils complicates handling of the droplets since these would float on the fluid since the water droplets would be less dense. This can cause aggregation and coalescence of the droplets. Here, we report the synthesis, characterization, and use of fluorinated polysiloxane oils that have densities similar to the one of water at room temperature, and when mixed with non-ionic fluorinated surfactants, can produce droplets encapsulating biochemical reactions. We show how droplets in these emulsions can host many biological processes, including PCR, DNA origami, rolling circle amplification (RCA), and Taqman® assays. Some of these use unnatural DNA built from an Artificially Expanded Genetic Information System (AEGIS) with six nucleotide "letters".

Introduction

There is a growing interest in the biochemical sciences for the compartmentalization or miniaturization of reactions [1, 2]. When conducted in water-in-oil droplets, compartmentalization allows experimentalists to run millions of reactions in parallel, creating ample opportunity to analyze the vast diversity contained within a biochemical sample. One can amplify an isolated gene in a digital PCR or explore the vast protein sequence space in directed evolution experiments [3]. Approaches such as directed evolution and/or high throughput screening require sequence diversity. These kinds of experiments require to isolate variants of a biomolecule. In some cases, enzymes can be isolated with their encoding genes and can be, considered by some, as forming a sort of "artificial cell". One way to achieve this compartmentalization and screening is with the use of water-in-oil droplets [4]. These "artificial cells" [5, 6] and other compartments have several applications, including drug delivery [7–9], enzyme directed evolution [1, 10–14], and models for the origin of life [15–19]. While water-hydrophobe-water systems are analogs of natural cells [20–25], simple water-in-oil emulsions are intrinsically easier to assemble and more stable to environmental change (especially heating) as compartment analogs of cells.

As with standard cells, compartments can maintain a link between the structures of molecules inside the droplet (the "phenotype") and the structures of the molecules that encode them (the "genotype"). This is important when experimentalists seek to direct the evolution of nucleic acids and their encoded proteins under selective pressure. For example, compartmentalization in two-phase artificial cell systems has been used for directed evolution [3] in the form of "compartmentalized self replication" (CSR). Developed by Tawfik and Griffiths, CSR holds proteins and genes together in water droplets suspended in oil emulsions [26]. CSR was applied to the directed evolution of DNA polymerases by Holliger and his collaborators [10]. CSR has also been used to select DNA polymerases that accept unnatural nucleotides [12, 27].

Compartmentalization is of great interest to synthetic biologists, who seek to put alien "xeno" nucleic acids (xNAs) into artificial cells. One example of xNA are artificially expanded genetic information systems (AEGIS) that increase the number of independently replicable nucleotides from 4 to as many as 12 [28]. By shuffling hydrogen bonding patterns of the G:C and A:T pairs while retaining their Watson-Crick size-complementarity [28]. AEGIS DNA can evolve to produce aptamers molecules that bind to liver and breast cancer cells [29] and isolated proteins [30]. Modified nucleic acids can potentially be used as therapeutics [31]; recently some AEGIS components have been suggested as potential inhibitors of the RNA polymerase from SARS-CoV-2 [32]. The Z:P pair from AEGIS used in this work is shown in Fig 1.

Compartmentalization in water-in-oil droplets requires a fluid immiscible with water and a surfactant. The surfactant must lower the surface tension of the liquid, stabilize the emulsion, and diminish coalescence [33, 34]. There are several commercially available surfactants and fluids for this purpose; however, there are some difficulties with these. For instance, in our laboratory, Span® 80 has been used to produce water-in-oil droplets, but we have known for years that there are observable differences between batches of the same product (S1 Fig in S3 File) potentially arising from the fact that it is derived from animal fat. In our experience, directed evolution experiments using Span80® proved unreliable. We have observed dark precipitates at the bottom of bottles of Span80® and in oil phases with Span80®-based mixtures (S2 Fig in S3 File). Furthermore, the same authors who pioneered the use of Span® 80 for creating water-in-oil droplets have reported the presence of contamination with peroxides [35, 36], which interferes with some biochemical processes. To counter these issues, silicone fluids were proposed as an alternative. There are many examples of research done with silicone fluids that come from the cosmetic industry. Some, commercialized by Degussa (now Evonik), are not available commercially in
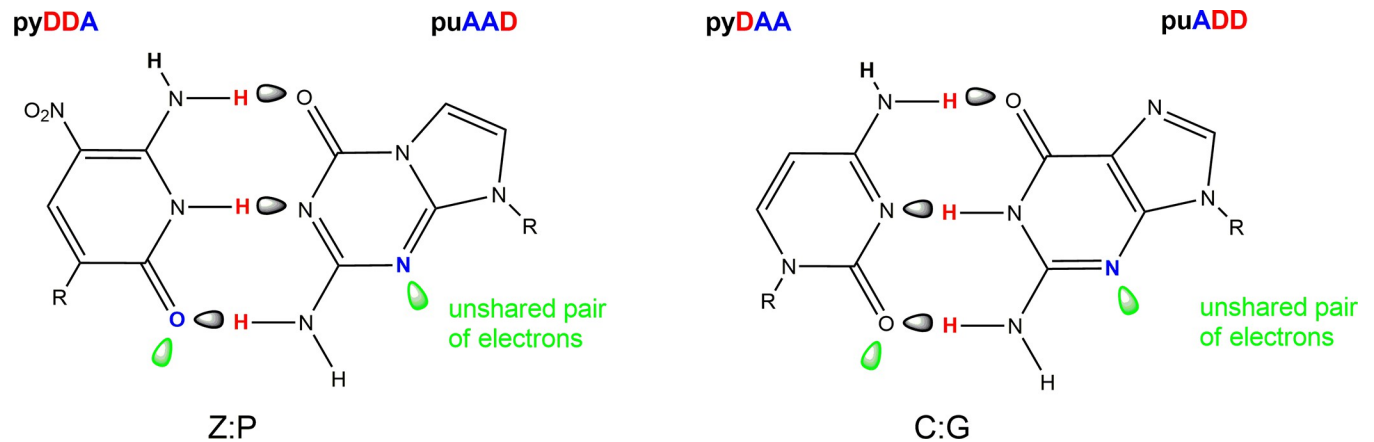
Fig 1. The Z:P pair from an Artificially Expanded Genetic Information System (AEGIS), left. AEGIS nucleotides follow the geometry and hydrogen bonding architecture of the natural nucleotides. The hydrogen bonding patterns are named pu or py, depending on whether they are presented on a large (purine-like) or small (pyrimidine-like) heterocyclic ring system respectively. Hydrogen bond donor (D) and acceptor (A) groups listed starting in the major groove and ending in the minor groove. Unshared pairs of electrons presented to the minor groove are shown in green orbitals. The Z:P pair presents the pyDDA:puAAD hydrogen bonding pattern, while the analog C:G pair presents the pyDAA:puADD hydrogen bonding pattern. R is deoxyribose.

research-sized amounts. One cannot expect that a batch of a silicone fluid to be used for producing sunscreen would go through testing for its suitability for PCR. For example Diehl *et al.* report the use of ABIL WE09 from Degussa for water-in-oil emulsions but notes in the supplementary section that dark precipitates are observed [37]. Not surprisingly some researchers fail to replicate the protocols published by other groups or at least need to modify some of the protocols [1]. The lack of more choices of surfactants for biotechnology have motivated other researchers to create their own biocompatible surfactants as well [38].

There are several commercially available fluorinated fluids, which are used for microfluidics. Fluorinated fluids have peculiar properties; they are immiscible with water and hydrocarbons, forming a third "flourous" phase. As natural proteins, membranes, and other biomolecular systems exploit both hydrophilic and hydrophobic phases, a purely hydrophobic oil or surfactant can disrupt biological systems because the hydrophobic portion of the surfactants can invade the hydrophobic cores of proteins and other biologics, disrupting their function. The fluorous phase comprising fluorinated species is sufficiently "orthogonal" to both hydrophilic and hydrophobic systems as to render that third phase inert with respect to most biological molecules systems containing them. Thus, fluorinated oils are used for drug delivery [39, 40], blood substitutes [41, 42], and diagnostics [43]. Several fluorinated oils and surfactants are now commercially available for water-in-oil emulsions, and several of these are widely used. These, however, have densities considerably higher than water, so the water droplets float, which makes it difficult to manipulate them for instance for re-injection. For example, the fluorinated oil HFE-7500 has a density of ~ 1.6 g/mL [44, 45]. Fluorinert® FC40 has a density between 1.845 and 1.895 [46–48]. Concentration of the droplets in the top of the fluid also increases the number of droplet-droplet encounters, which encourages droplet fusion.

These considerations provided the motivation to seek fluorinated oils that have a density close to 1 g/mL, the density of aqueous solutions in which biological processes act. The synthesis of silicones from hexamethylcyclotrisiloxane by ring-opening polymerization has been reported before [49]. We report here the synthesis, characterization of polysiloxanes, prepared by ring-opening polymerization under conditions that produce fluids with densities near 1 g/mL while having enough fluorinated monomers to be able to dissolve non-ionic fluorinated surfactants that enable their use for the encapsulation of biochemical reactions.

Materials and methods

Materials

Hexamethylcyclotrisiloxane, 1,3,5-trimethyl 1,3,5-tris(3,3,3 trifluoropropyl) cyclotrisiloxane, and 2,4,6,8-tetramethylcyclotetrasiloxane were purchased from Changzhou Fluoride Chemical Co. Genuine Technology. Hexamethyldisiloxane was purchased from Acros. Amberlyst® 15 hydrogen form and potassium trichloro(ethylene) platinate (II) hydrate were purchased from Sigma-Aldrich. Nonafluorohexyldimethylchlorosilane, 3,3,3 trifluoropropyldimethylchlorosilane; allyloxy(polyethylene oxide) (4–7 EO); allyloxy(polyethylene oxide), methyl ether (6–8 EO) were obtained from Gelest. All chemicals were used without purification. Oligos containing artificial nucleotides, artificial triphosphates dZTP, dPTP were obtained from Firebird Molecular Biosciences. Phi29 polymerase and Exonuclease I were purchased from New England Biolabs. CircLigase™ was purchased from Lucigen. Snap-Cap Microcentrifuge Biopur™ Safe-Lock™ or Safe-Lock Tubes 2 mL were from Eppendorf™. Stainless steel balls, 6 mm were obtained from IKA. EvaGreen® Dye 20X in water was from Biotium. For DNA origami: a "Folding kit basic p7249 Cuboid with large aperture" was obtained from Tilibit Nanosystems. All natural DNA oligos and fluorescent probes were obtained from IDT.

Ring-opening polymerization

Polysiloxanes were prepared by the ring-opening reaction shown on Fig 2. Two different protocols were developed:

Protocol 1.   The fluorinated monomer 1,3,5-trimethyl 1,3,5-tris-(3,3,3-trifluoropropyl)-cyclotrisiloxane (12 g; 25.6 mmol) was mixed with the non-fluorinated monomer hexamethyl-cyclotrisiloxane (72 g; 323.7 mmol) and hexamethyl disiloxane (3 mL; 14.1 mmol); the second acted as a chain terminator. The mixture was heated to 75˚C in an oil bath. Amberlyst® 15 catalyst (1.2 g) was added once the reaction mixture was homogeneous. The reaction proceeded under argon for 3 hours at 75˚C. Once cooled, the reaction mixture was decanted from the solid Amberlyst® catalyst.

The products were then resolved by distillation under reduced pressure (23 mm Hg). Unreacted materials were removed at 90˚C while collecting a fraction of the fluorinated fluid. After removing materials at 90˚C; the remaining fluid was labeled as Fluid A. From this fluid a low molecular weight (LMW, Fluid B) fraction was obtained by distillation (150˚C, 23 mm Hg); a high molecular weight fraction remained, non-distilled (HMW fraction).

Protocol 2.   The fluorinated monomer 1,3,5 trimethyl 1,3,5-tris(3,3,3-trifluoropropyl) cyclotrisiloxane (25.26 g; 53.9 mmol) was mixed with the non-fluorinated monomer, hexamethylcyclotrisiloxane (36 g; 161.8 mmol) and hexamethyl disiloxane (2.8 mL; 13.11 mmol). The mixture was heated to 75˚C in an oil bath. Catalyst Amberlyst® 15 (1.2 g) was added last, again after the mixture was homogeneous. The reaction proceeded under argon for 4 hours at 75˚C. Then, an opaque liquid was decanted to separate it from the solid catalyst. Distillation using a Kugelrohr apparatus (90˚C, 23 mm Hg) removed unreacted starting materials. This remaining fluid was left at room temperature for 8 hours, after which it had separated into two layers each with different characteristics (top layer: fluid C; bottom layer: fluid D).

Fluorinated surfactants

Fluorinated hydrophilic chains were synthesized following the work of Kobayashi and Owen [50]. Two fluorinated hydrophobes have been explored: 3,3,3-trifluoropropyl (Pr_f) and 3,3,4,4,5,5,6,6,6-nonafluorohexyl (Hx_f). These hydrophobes were combined with allyloxy(polyethylene oxide) following reference [50] with some modifications. The surfactants (Fig 3) were
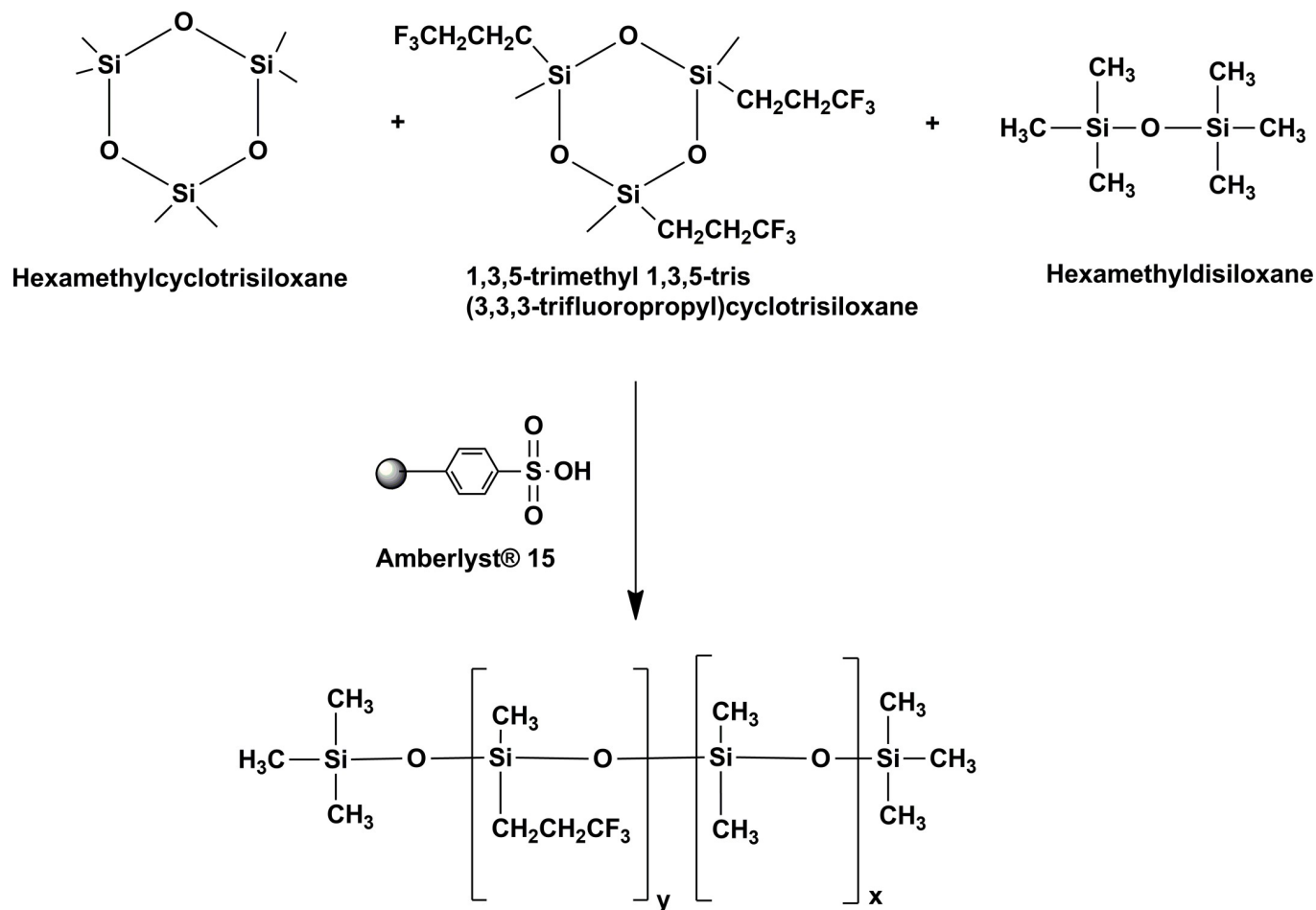
Fig 2. Ring-opening polymerization used to produce the fluorosilicone fluid. The two cyclotrisiloxane monomers (hexamethylcyclotrisiloxane and 1,3,5-trimenthyl 1,3,5-tris(3,3,3-trifluoropropyl)cyclotrisiloxane) are reacted along with hexamethyl disiloxane, which acts as a chain terminator. The catalyst Amberlyst® 15 acts as an acid catalyst for the ring-opening reaction.

prepared by hydrolysis of their chlorosilane precursors and eventually bound to the hydrophile by hydrosilation with allyloxy(polyethylene oxide). A scheme of the synthesis and details are provided in the supplementary information section (S3 Fig in S3 File).

Gel permeation chromatography

Gel permeation chromatography (GPC) was performed by Cambridge Polymer Group (Boston, MA) using an Agilent 1100 Series HPLC Gel Permeation Chromatogram equipped with an autosampler, thermostatted column oven, and refractive index detector. The column used for the separation was the Agilent PLgel Mixed-B column (10 μm particle size; 300 mm X 7.5 mm) which has a nominal linear molecular weight separation range from 500–10,000,000 g/mol. These columns are packed with a stationary phase consisting of ~10 μm gel particles which are composed of a highly crosslinked polystyrene/divinylbenzene matrix. These columns are organic GPC columns, compatible with most organic mobile phase solvents.

Data collected by refractive index (RI) detection was used for characterization of the molecular weight distribution, molecular weight moments, and polydispersity of the samples. The data were analyzed using the Agilent GPC/SEC software v A.02.01. A calibration curve was
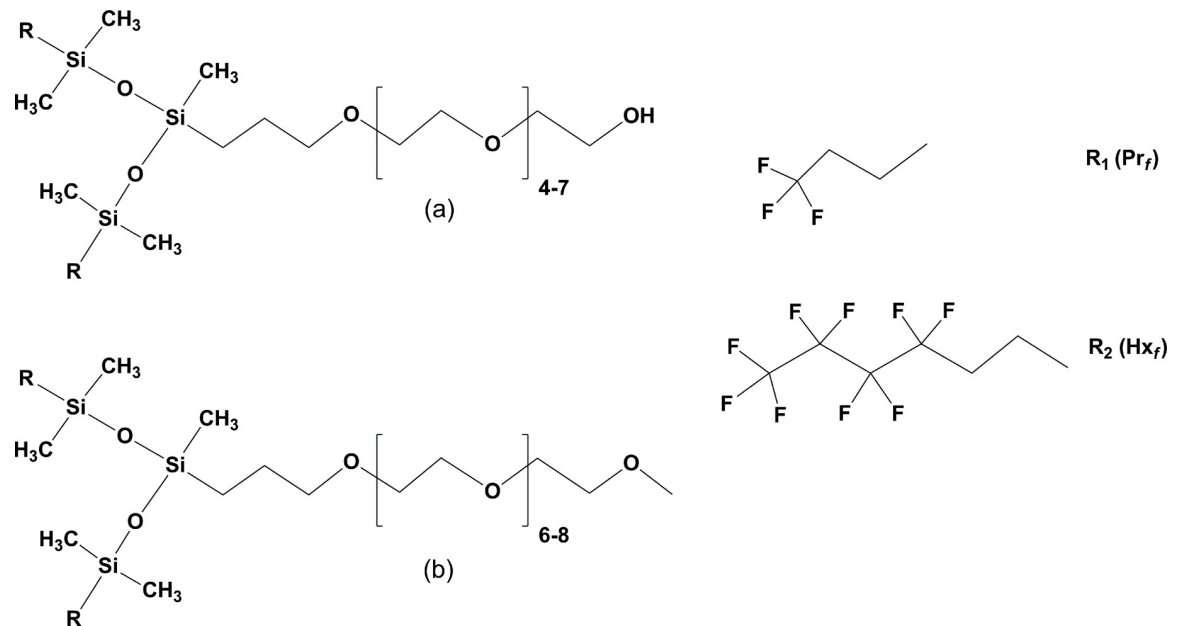
Fig 3. Nonionic fluorosilicone surfactants. The amphiphilic molecules are produced by reacting SiH functionalized branched disiloxanes hydrophobes with allyloxy(polyethylene oxide) following reference [50]. Two different hydrophiles (a, b) and two hydrophobes are shown: one with the 3,3,3-trifluoropropyl (R_1, Pr_f) and 3,3,4,4,5,5,6,6,6-nonafluorohexyl (R_2, Hx_f).

prepared using polystyrene standards with molecular weights between approximately 500 and 10,000,000 g/mol. A measured amount of the material was transferred to a glass vial with a PTFE lined screw cap. An amount of toluene sufficient to produce a sample concentration of 5 mg/ml was added to each sample, which were then mixed using gentle agitation at a temperature of 30°C overnight. All samples were clear and colorless. The samples were filtered through 0.45 µm PTFE syringe filters into autosampler vials, filled to the shoulder. Three autosampler vials were prepared of the samples for triplicate injection purposes. Molecular weight moments and polydispersity index (PDI) were calculated by Agilent GPC/SEC Software (v A.02.01) as:

$Mn = \Sigma M_i N_i / \Sigma N_i$

Where Mn is the number molecular weight; M_i is the molecular weight of a chain and N_i is the number of chains of that molecular weight.

$Mw = \Sigma M_i^2 N_i / \Sigma M_i N_i$

Mw is the weight average molecular weight. In this molecular weight value the more massive chains contribute more to the molecular weight average.

$PDI = Mw/Mn$

PDI is the polydispersity index.

Origami DNA

The origami folding mixture comprised 208 staples, each 200 nM (S1 Table in S3 File) and a scaffold (20 nM), which was a single-stranded DNA p7249 isolated from M13mp18 (7,249 nucleotides) in Tris buffer (5 mM, pH ~ 8.2, with 1 mM EDTA, 20 mM MgCl$_2$, and 5 mM NaCl.

Droplet formation was done using PDMS radial chips that empty droplets of aqueous phase from 20 µm channels into an annular oil flow channel of 50 µm, as previously described by Paegel and Joyce [10]. The continuous phase was a 2% (v/v) of a fluorinated surfactant (a-R_2)

in Fluid B. The continuous phase was pumped at a rate of 5 μL/min while the aqueous phase was pumped at a rate of 7 μL/min.

The origami mixture, both bulk (as a positive control) and emulsified, were placed in a thermal cycler at 65°C for 10 minutes and then cooled to 60°C at 0.1° C/s. After this hold, the temperature was lowered by 0.5°C steps (0.1°C/s rate) and held at the new temperature for 30 minutes until 40°C was reached. At the end of the cooling steps the emulsion was centrifugated for 5 minutes at 5,000 xg. Then, 25 μL of the origami reaction were mixed with the provided 6X loading buffer provided with the kit and loaded in an agarose gel 0.5 X Tris-borate EDTA buffer with ethidium bromide and 6 mM $MgCl_2$.

Six-nucleotide PCR with Artificially Expanded Genetic Information Systems (AEGIS)

An aqueous solution holding all components required for a PCR was prepared, consisting of: (a) primers (20 nM each) 5'- GACGGACTGCCTATGAG-3 and 5'-GAGGCGATCGCAGTA TC-3'; (b) double stranded template (2×10^{-7} μM):

5'- GACGGACTGCCTATGAGCAGTT**Z**AAAAG**Z**TATGATACTGCGATCGC CTC-3' and 5'- GAGGCGATCGCAGTATCATA**P**CTTTTT**P**AACTGCTCATAGGCAGTCCGTC-3'; (c) substrates, dNTPs, dZTP, and dPTP (0.2 mM each), (d) Evagreen 2X; (e) a variant of *Taq* DNA polymerase fused to the DNA binding protein of *Sulfolobus solfactaricus* Sso7d-*Taq*(Δ1–280) [R587Q E626K I707L E708K A743H E832G]) at 7.1×10^{-2} μM; and (f) buffer, with 20 mM Tris-HCl, pH 8.4; 10 mM $(NH_4)_2SO_4$; 10 mM KCl; 2 mM $MgSO_4$; 0.1% Triton® X-100.

The PCR mixture (100 μL) was emulsified along with 300 μL of a fluorinated fluid with density 1.009 g/mL that contained 2% (v/v) surfactant (a-R_2). The fluid was prepared by mixing 1 mL of fluid B with 4 mL of the HMW fluid (protocol 1). The mixture of two phases was placed in a Safe-Lock Tube with and a 6 mm stainless steel bead. The tube was then fitted in a 96-well storage plate and secured between the top and bottom plates of TissueLyser II (QIAGEN). The components were then mixed for 10 seconds at 15 Hz followed by 7 seconds at 17 Hz. Then, 50 μL of emulsion were transferred to PCR tubes with an optical lid by triplicate. The PCR used the following cycle: 92°C for 30 seconds 40 cycles: [92°C for 10 seconds; 48°C for 15 seconds; 72°C for 20 seconds] and acquired fluorescence after each cycle using a Lightcycler® 96 (Roche Life Science).

Taqman® assay in droplets

An aqueous solution containing the components of a Taqman® assay reaction was prepared to contain:

- Template: 5'-CAGCAGTGCCAGCAGAACAAAGGTATTCATCTTAGTGA**P**GTGCGC AGTCAGCTCACTACT-3', at 0.4 μM concentration.

- Primer: 5'-AGTAGTG AGCTGACTGCGC-3', at 0.2 μM concentration; and

- Probe: 5'- FAM-ATGAATACC-ZEN-TTTGTTCTCTGCTGG CAACTGCTG-3'

The other components of the reaction mixture were: (a) substrate dNTPs and dZTP, each at 0.2 mM; (b) buffer at 10 mM Tris pH 8.3, 1.5 mM $MgCl_2$, 50 mM KCl; and (c) enzyme, a variant of *Taq* DNA polymerase [R587Q, E832C], 6 pmol/50 μL reaction.

The aqueous mixture (100 μL) was emulsified along with 300 μL of a fluorinated fluid with density 1.009 g/mL that contained 2%(v/v) surfactant (a-R_2). The fluid was prepared by mixing 1 mL of fluid B with 4 mL of the HMW fluid (protocol 1). The tube containing the two phases was then fitted in a 96-well storage plate and secured between the top and bottom plates of

TissueLyser II (QIAGEN). The components were then mixed for 10 seconds at 15 Hz followed by 7 seconds at 17 Hz. Then, 50 μL of emulsion were transferred to PCR tubes with an optically clear lid and placed in the following cycle: 40 cycles of: [95˚C for 8 seconds; 62˚C for 24 seconds] and acquired fluorescence after each cycle using a Lightcycler® 96 (Roche Life Science).

Rolling Circle Amplification (RCA) in droplets

An aqueous mixture comprising all of the components for a RCA reaction was prepared to include: 1X Phi29 buffer (New England Biolabs), which has 50 mM Tris-HCl at pH 7.5, 10 mM $MgCl_2$, 10 mM $(NH_4)_2SO_4$, and 4 mM DTT (@ 25˚C); (b) triphosphates, dATP, dCTP, dTTP, dGTP, 0.2 mM each; primer at 0.8 μM, having the sequence 5ʹ-CAGGGCTGGGCATA GAAGTCAGGGCAGA-3ʹ; polymerase, Phi29 0.1 U/μL, with BSA 0.2 μg/μL; circular ssDNA template molecule at 2.5 μg/μL. The circular ssDNA template was prepared by circularizing: P-5ʹTATGCCCAGCCCTGTA AGATGAAGATAGCGCACAATGGTCGGATTCTCAACTCG TATTCTCAACTCGTATTCTCAACTCGTCTCTGCCCTGACTTC-3ʹ with CircLigase™ (Lucigen) according to the manufacturer protocol. Non-circularized material was degraded with Exonuclease I (*E. coli*) according to the manufacturer protocol as well.

The aqueous mixture holding all the components necessary for RCA was emulsified by placing aqueous mixture (100 μL) along with 300 μL of a fluorinated fluid with density 1.009 g/mL that contained 2%(v/v) surfactant (a-R_2). The fluid was prepared by mixing 1 mL of fluid B with 4 mL of the HMW fluid (protocol 1). The tube containing the two phases was then fitted in a 96-well storage plate and secured between the top and bottom plates of TissueLyser II (QIAGEN). The components were then mixed for 10 seconds at 15 Hz followed by 7 seconds at 17 Hz. Then, 50 μL of emulsion were transferred by triplicate to PCR tubes with an optically clear lid. Fluorescence was acquired after each minute using a Lightcycler® 96 (Roche Life Science).

Expression and purification of the DNA polymerase variants. A plasmid (pJExpress414, DNA 2.0) containing the gene encoding the *Taq* DNA polymerase variant of interest was expressed in *E. coli* C43(DE3) (37˚C, overnight growth, IPTG 0.5 mM) in LB media (50 mL). The next morning, cells were pelleted (~ 0.75 g) in a refrigerated centrifuge for 10 minutes at 5,000 x g and stored at -20˚ C. The pellet was resuspended in 2.5 mL of Tris 50 mM; glucose 50 mM; EDTA 1 mM; pH 8.0 and heat-shocked at 75˚C for 10 minutes, then mixed with 3.75 mL of BugBuster® master mix (Novagen) for 20 minutes at room temperature. The lysate was pelleted in 1.5 mL tubes, at 21,000 xg for 5 minutes and the supernatant was mixed with NiNTA resin (1.5 mL of resuspended resin washed and resuspended in 4 mL of Lysis buffer: Tris HCl, 20 mM pH 8.0; NaCl 500 mM, imidazole 10 mM). The lysate and the resin were then incubated and gently spun at 4˚C for 1 h.

The lysate was then loaded on a column and washed with: (a) 2 mL wash: Tris, 20 mM; NaCl, 1 M; followed by (b) 1 mL wash: Tris, 20 mM; NaCl, 150 mM; followed by (c) 2 mL wash: Tris, 20 mM; NaCl, 500 mM; imidazole, 20 mM; and (d) eluted with elution buffer: 1 mL Tris HCl, 10 mM, pH 8.0, NaCl 250 mM, imidazole 500 mM. Buffer was exchanged by ultracentrifugation (AMICON, 15 mL, 50,000 MW cutoff) to final storage buffer, which was 10 mM Tris pH 8.0; 100 mM KCl; 0.5 mM DTT; 0.1 mM EDTA; 0.5% Tween 20; 0.5% Igepal; glycerol 50%. Protein concentration was measured using Pierce™ BCA Protein Assay Kit, following the manufacturer recommendations.

Results

Fluorine has an atomic mass of 19, meaning fluorinated molecules are intrinsically denser than water. However, this greater atomic mass can be partly offset by the larger mean volumes

of CF$_2$ (38 Å^3) and CF$_3$ (92 Å^3) groups relative to CH$_2$ (27 Å^3) and CH$_3$ (54 Å^3) [31], both less dense than water. Therefore, we reasoned that fluorous oils having a density of water might be obtained by balancing their fluorinated components with alkane components. This balancing must also consider the density of silicon (Si = 28 g/mole) since cyclotrisiloxanes are part of the polymerization mixture.

With these considerations, we explored methods to prepare low-density fluorous oils by reacting siloxanes having both alkane and trifluoromethylalkane side chains, specifically 1,3,5-trimethyl 1,3,5-tris(3,3,3-trifluoropropyl)-cyclotrisiloxane and hexamethylcyclotrisiloxane (Fig 2). It was taken into consideration that the growth of the polymeric chain must be limited since high molecular weight molecules will increase the viscosity of the fluid. For this purpose the chain termination component (hexamethyldisiloxane) plays an essential role.

Ring-opening polymerization

Acid-catalyzed ring-opening polymerization following protocol 1, produced polysiloxanes with bimodal molecular weight distribution (Fig 4). Protocol 2 produced two fluids with different densities which spontaneously separated. Interestingly, each of these fluids exhibits a bimodal molecular weight distribution as well (Fig 5). Following protocol 1, fluid A was separated by distillation using a Kugelrohr apparatus. Obtaining 15 mL of the lower molecular
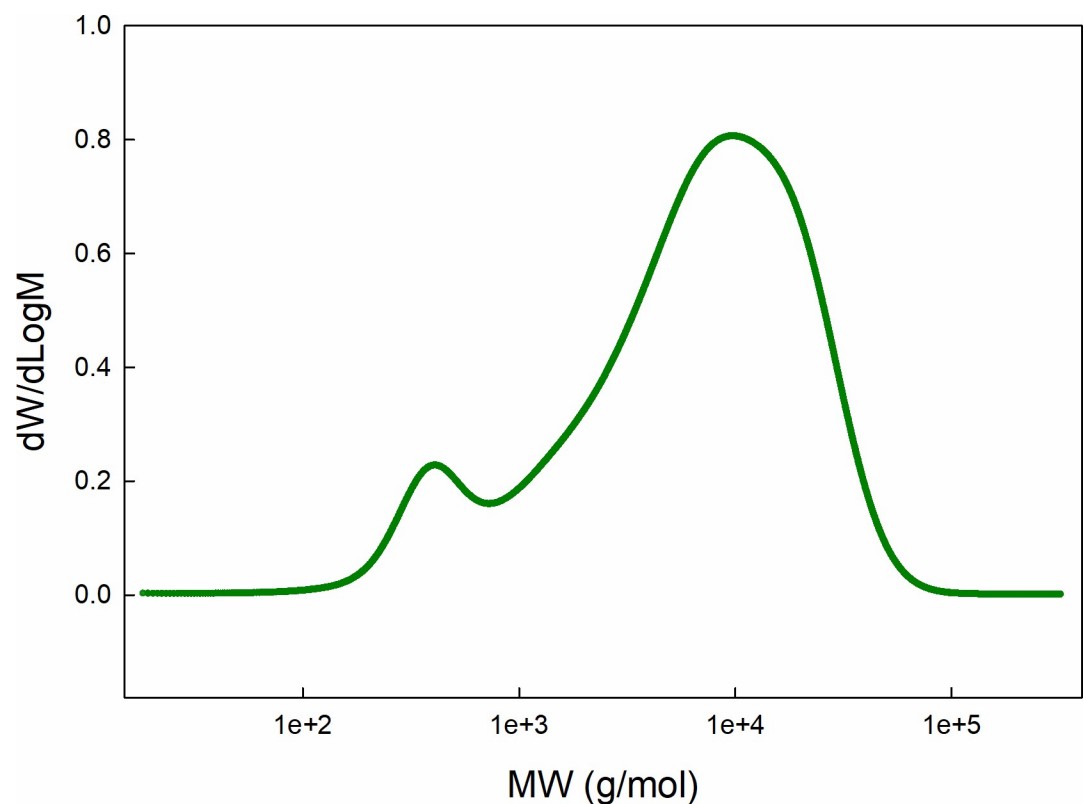

Fig 4. Molecular weight distribution of polysiloxanes produced via protocol 1. Ring-opening polymerization following "protocol 1" produced polysiloxanes with bimodal distribution. These two peaks can be separated by distillation under reduced pressure with a high molecular weight peak (Mp ~ 9,400 g/mol) and a low molecular weight peak (Mp ~ 300 g/mol). The low molecular weight fraction contains a higher concentration of fluorinated monomers estimated by ^{1}H-NMR and is capable of dissolving the fluorinated surfactants. Peak 1 corresponds to the higher molecular weight peak (rightmost) and peak 2 corresponds to the lower molecular weight peak (leftmost). S4 Fig in S3 File. shows an overlay of two gel permeation chromatography runs of the two distinctive fractions separated by distillation.
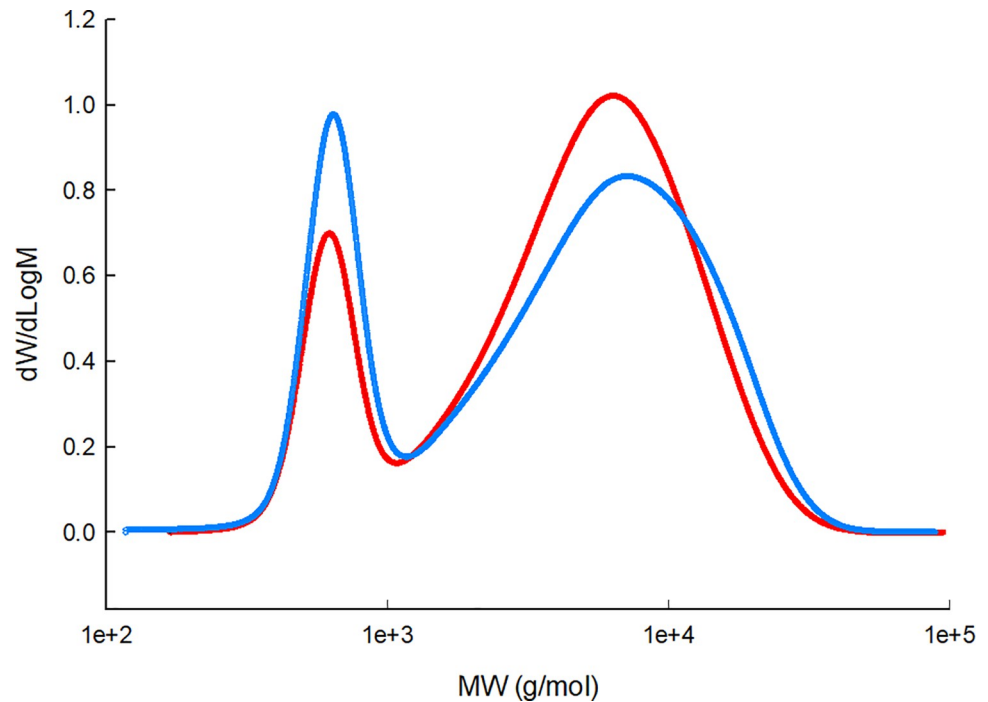
https://doi.org/10.1371/journal.pone.0252361.g004

Fig 5. Molecular weight distribution of polysiloxanes produced via protocol 2. Ring-opening polymerization following "protocol 2" produced two liquid polysilioxanes that spontaneously separate in two phases with different densities and are referred as fluid C (red) and fluid D (blue). Each fluid exhibits bimodal molecular weight distribution.

https://doi.org/10.1371/journal.pone.0252361.g005

weight fraction (150˚C, 23 mm Hg) with a density of 1.0565 g/mL. The remaining fluid (~ 53 mL) consists of a high molecular weight fraction with density 1.031 g/mL; this remained undistilled up to 200˚C at 23 mm Hg). Table 1 lists molecular weight values for different fractions.

Reported molecular weight moments and polydispersity from the overall chromatogram, as average +/- one standard deviation. Molecular weights are reported in polystyrene equivalents. Fluid A peak 1 is referred as high molecular weight fraction (HMW) and Fluid A peak 2 referred as low molecular weight fraction (LMW). $Mn = \Sigma M_i N_i / \Sigma N_i$, where Mn is the number molecular weight; M_i is the molecular weight of a chain and N_i is the number of chains of that molecular weight. $Mw = \Sigma M_i^2 N_i / \Sigma M_i N_i$, where Mw is the weight average molecular weight. In

Table 1. Summary of molecular weight moments and polydispersity.

sample	Mp [g/mol]	Mn [g/mol]	Mw [g/mol]	PDI
Fluid A	9,404 ± 57.7	1748 ± 31.2	10,126 ± 83.5	5.793 ± 0.058
Fluid A peak 1	10,321 ± 34.6	3,206 ± 486	11,478 ± 74.0	3.637 ± 0.561
Fluid A peak 2	321 ± 2.08	230 ± 2.65	305 ± 2.00	1.326 ± 0.008
Fluid C	6,412 ± 64	2,064 ± 11	6,266 ± 116	3.04 ± 0.06
Fluid C peak 1	6,412 ± 64	4,549 ± 34	7,529 ± 144	1.66 ± 0.019
Fluid C peak 2	626 ± 6	597 ± 3	637 ± 3	1.07 ± 0.008
Fluid D	645 ± 4	1,722 ± 12	6,543 ± 119	3.80 ± 0.07
Fluid D peak 1	7,178 ± 47	4,892 ± 23	8,522 ± 70	1.74 ± 0.009
Fluid D peak 2	645 ± 4	611 ± 4	661 ± 4	1.08 ± 0.003

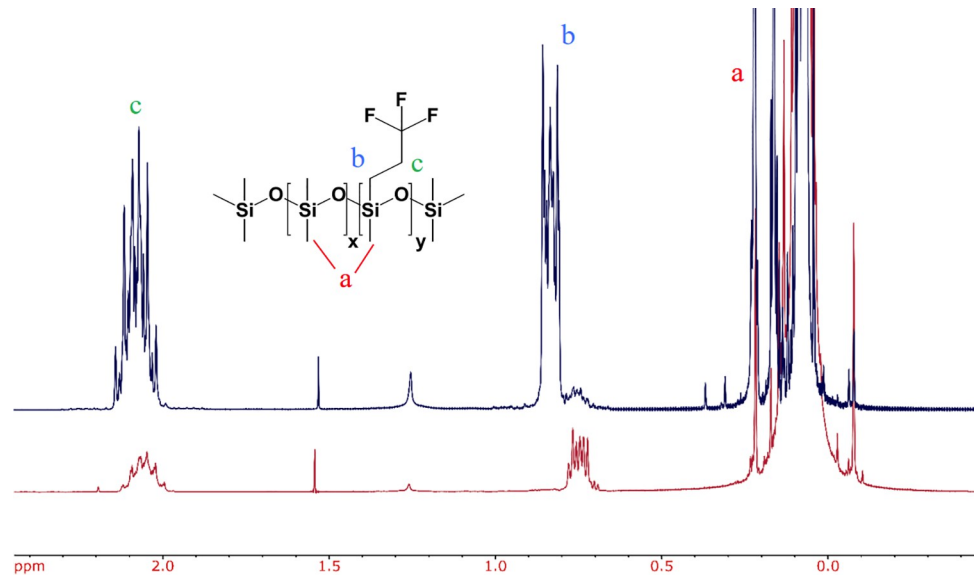https://doi.org/10.1371/journal.pone.0252361.t001

Fig 6. [1]NMR analysis of fluorosilicone polysiloxanes. Overlay of the ^{1}HNMR of the low molecular weight (blue) and the high molecular weight (red) fraction samples indicating the assigned peaks.

https://doi.org/10.1371/journal.pone.0252361.g006

this molecular weight value the more massive chains contribute more to the molecular weight average. PDI is the polydispersity index. PDI = Mw/Mn.

^{1}HNMR analysis. Resonances with chemical shifts between 0.0 and 0.3 ppm were assigned to Si-CH$_3$ (labeled "a" in Fig 6). These signals arise from both fluorinated and non-fluorinated monomers. Resonances with chemical shifts between 0.7 and 0.9 ppm were assigned to the methylene groups attached to Si (α-CH$_2$-, labeled "b" in Fig 6). Resonances with chemical shifts between 1.9 and 2.2 ppm were assigned to the methylene beta to the Si (β-CH$_2$-, labeled "c" in Fig 6) for the fluorinated monomers that contained -CH$_2^{\alpha}$-CH$_2^{\beta}$-CF$_3$.

The ratios of non-fluorinated monomer to fluorinated monomer were calculated using the integrals from the β protons (denoted by "c") and the Si-CH$_3$ protons (denoted by "a"). The following equation was used to determine the monomer ratio:

$$\frac{\text{Non} - \text{fluorinated monomer}}{\text{Fluorinated monomer}} = \frac{(A_a - 3)/6}{A_c/2}$$

Here, A$_c$ is the integration area of the peak for the β-CH$_2$- protons and A$_a$ is the integration area of the peak for the Si-CH$_3$ protons. The integration values and monomer ratios are summarized in Table 2.

The integral of the resonances assigned to the Si-CH$_3$ units (0.0 to 0.3 ppm) is inversely proportional to the fraction of fluorinated monomers present in the fluid. It was observed that

Table 2. Integration of peaks used for determination of the ratio of non-fluorinated monomer: Fluorinated monomer.

Sample	β-CH$_2$	Si-CH$_3$	non-fluorinated monomer: fluorinated monomer
Fluid A peak 2 (LMW)	2	18.3	2.6: 1
Fluid A peak 1 (HMW)	2	96.3	15.6: 1

Values for samples HMW: high molecular weight and LMW: low molecular weight. ^{1}HNMR **β-CH$_2$** integral was set to the value 2. ^{1}HNMR data is representative of several trials.
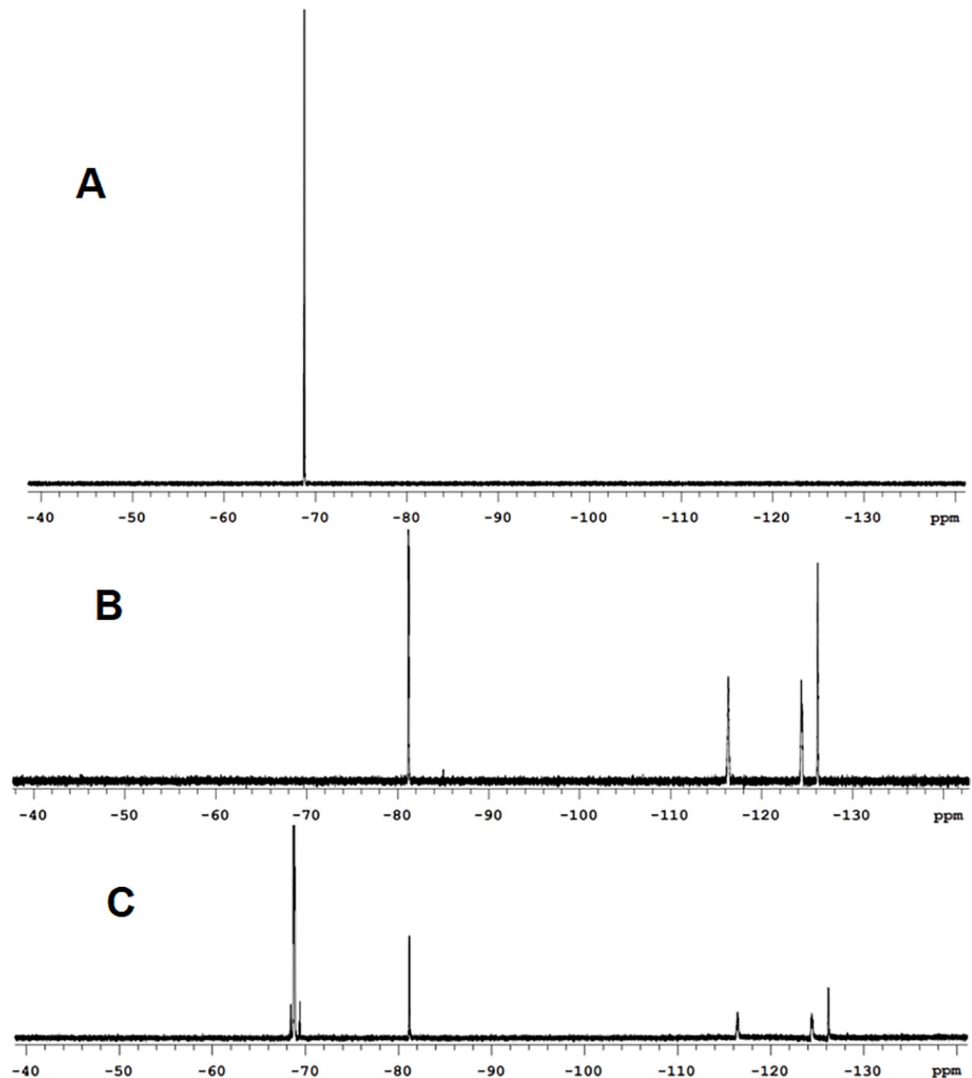
https://doi.org/10.1371/journal.pone.0252361.t002

Fig 7. ^{19}FNMR overlays showing the presence of the surfactant with the Hx$_f$ hydrophobe CF$_3$CF$_2$CF$_2$CF$_2$CH$_2$CH$_2$- dissolved in the low molecular weight fluid (fluid B). (A) A single peak that comes from the CF$_3$CH$_2$CH$_2$- from the fluorinated fluid. (B) Four peaks that correspond to the fluorine of the Hx$_f$ hydrophobe CF$_3$CF$_2$CF$_2$CF$_2$CH$_2$CH$_2$-. (C) ^{19}FNMR of a homogeneous 4% solution (v/v) of the surfactant in the fluorinated fluid exhibiting the signals from both components.

https://doi.org/10.1371/journal.pone.0252361.g007

fractions with higher fluorinated monomers exhibited lower viscosity. As expected, the fractions with a higher degree of fluorination were capable of solubilizing the nonionic fluorinated surfactants. Figs 7 and 8 show ^{19}FNMR and ^{1}HNMR of homogeneous solutions of the surfactants in the low molecular weight fraction (Fluid B, protocol 1). These solutions remained homogeneous for at least 10 days. The NMR spectra show the distinctive signals that arise from the surfactants solubilized to 4% (v/v). Table 3 shows different values of density, viscosity and proportion of non-fluorinated to fluorinated monomer compositions in the fluorinated polysiloxanes.

Droplet formation

Droplets shown in this work were made using two methods: using microfluidic devices or by shaking using a QIAGEN TissueLyser II. Fig 9 shows droplets produced with a radial
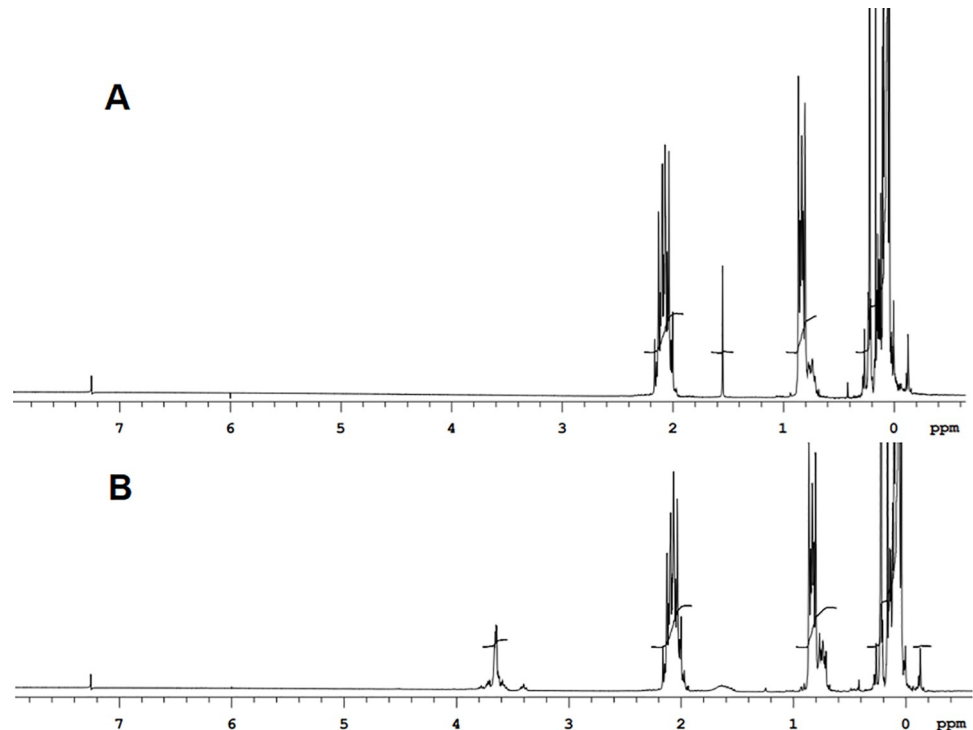
Fig 8. ^{1}HNMR overlays showing the presence of the surfactant with the Pr$_f$ hydrophobe CF$_3$CH$_2$CH$_2$- dissolved in the low molecular weight fluid (fluid B). (A) ^{1}HNMR of the fluid without surfactant. (B) ^{1}HNMR of a 4% (v/v the fluid with surfactant.A single peak that comes from the CF$_3$CH$_2$CH$_2$- from the fluorinated fluid. The characteristic signals of the -(CH$_2$CH$_2$-O)- can be observed at 3.4–3.8 ppm.

microfluidics chip. Fig 10 shows droplets formed by shaking 300 μL of the fluid/surfactant with 100 μL of the aqueous phase in a Safe Lock tube with a 6 mm stainless steel bead.

Next, we challenged the emulsions prepared with these fluid/surfactant mixtures to host processes that involve both DNA and enzymes, all useful in biomolecular sciences, nanotechnology: (a) Assembly of origami DNA nanostructures inside droplets suspended in the fluorinated oil. (b) PCR amplification of 6-letter DNA templates inside droplets suspended in the

Table 3. Viscosity, density and other properties measured on fluorinated polysiloxanes.

sample	density (g/mL)	Viscosity (cSt)	^{1}HNMR β-CH2 integral	^{1}HNMR Si-CH3 integral	MW (g/mol)	PDI	non-fluorinated: fluorinated monomer
Fluid A peak 2	1.031	n/d	2	18.3	305	1.3	2.55: 1
Fluid A peak 1	1.0565	n/d	2	96.3	11,478	3.6	15.55: 1
HMW fluid	0.986	67	2	58.0	10,126	5.8	9.17: 1
Fluid C	1.0457	6.06	2	33.98	6,266	3.04	5.16: 1
Fluid D	1.1347	10.8	2	12.24	6,543	3.8	1.54: 1
Fluid B *	1.1397	4.5	2	11.48	n/d	n/d	1.41: 1

Summarized viscosity and molecular weight analysis for fluorinated polysiloxane samples. Reported viscosity as fitted using a Newtonian model. Determined by Cambridge Polymer Group using a TA Instruments DHR-2 rheometer. Reported molecular weight moments and polydispersity from the overall chromatogram, as average +/- one standard deviation. Molecular weights are reported in polystyrene equivalents. Fluid B* was prepared following protocol 1 but with a shorter time of reaction obtaining a fluid with lower viscosity but with higher density and higher proportion of fluorinated monomers. ^{1}HNMR **β-CH$_2$** integral was set to the value 2. Some tests not performed are indicated as "not determined" n/d.
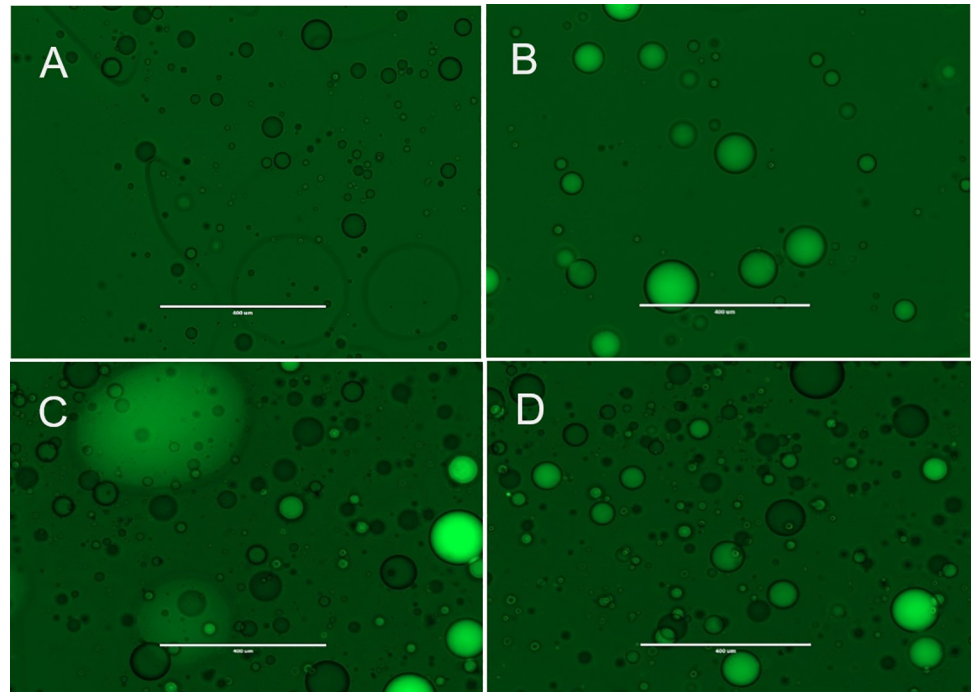
Fig 9. Transmission microscope images of droplets containing oligos with a FAM fluorescent molecule or a Black Hole Quencher (BHQ). The fluorinated fluid (fluid B) with 1% of surfactant (b-R_1) was pumped at 10 μL/min. Aqueous phase contained 5 μM of 5'-CTGCTCATAGG CAGTCCGTCA-BHQ-3' or 5'-FAM-TGACGGACTGCCTATGAGCAG-3' in 20 mM Tris-HCl, pH 8.4; 10 mM $(NH_4)_2SO_4$; 10 mM KCl; 2 mM $MgSO_4$; 0.1% Triton® X-100. Aqueous phase was pumped at 2 μL/min. (A) Droplets carrying oligo with Black Hole Quencher (BHQ). (B) Droplets carrying oligo with FAM. (C). Droplets carrying BHQ placed on the left side of the glass slide and droplets carrying FAM placed on the right hand side of the slide. (D) After being in contact for 10 minutes no fusion is observed. Scale bar is 400 μm. Pictures are representative of several trials.
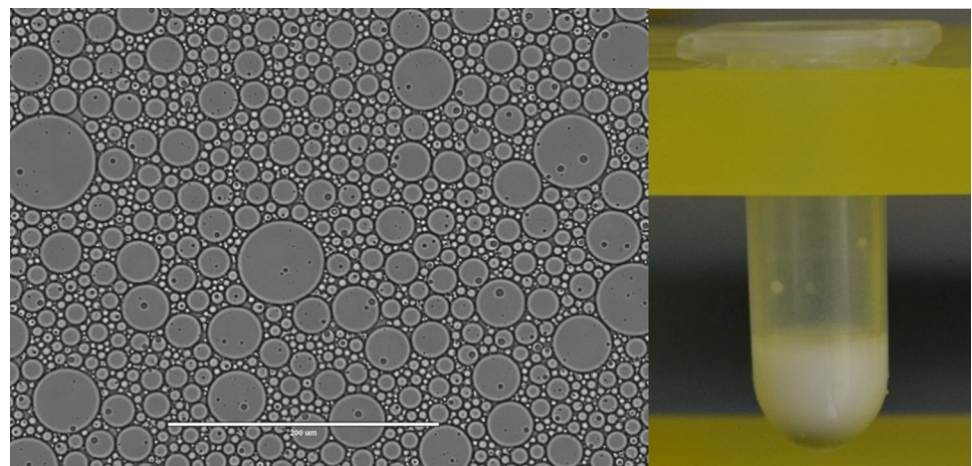
https://doi.org/10.1371/journal.pone.0252361.g009

Fig 10. Emulsion made with fluid C (protocol 2). Left: transmission microscope image of droplets. Scale bar is 200 μm. Right: picture of the emulsion formed by shaking 100 μL of buffer and 300 μL of fluid C with 2% of the surfactant a-R_2 containing the Hx_f hydrophobe. The emulsion is formed by shaking the contents in a Snap-Cap Microcentrifuge Biopur™ Safe-Lock™ Tube containing a 6 mm stainless steel bead. The tube was fitted in a TissueLyser II and shaken for 10 seconds at 15 Hz followed by 7 seconds at 17 Hz. Scale bar is 400 μm. Pictures are representative of several trials.

https://doi.org/10.1371/journal.pone.0252361.g010

fluorinated oil, including those built from an AEGIS DNA alphabet. (c) Generation of fluorescent signals inside droplets suspended in the fluorinated oil using a Taqman® assay, also with six-letter DNA real-time PCR.

(d) Generation of fluorescent signals inside droplets suspended in the fluorinated oil from the formation of RCA products.

Origami DNA

An origami kit obtained from Tilibit Nanosystems that assembles to form a cuboid of dimensions 61 nm x 8 nm x 52 nm with an aperture of 9 nm x 15 nm was set up as suggested by the manufacturer. The formation of the nanostructure was verified by its distinctive shift in migration compared with the scaffold when electrophoresed in a 2% agarose gel in 0.5 X TBE with ethidium bromide and 6 mM $MgCl_2$. The migration pattern of the scaffold DNA and a correctly assembled nanostructure is shown in S8 Fig in S3 File. The purified nanostructure has been characterized by Transmission Electron Microscopy (S9 Fig in S3 File). Our results showed that both the emulsified and non-emulsified origami reaction produced a nanostructure with the expected migration pattern (Fig 11). The result shown in Fig 11 comes from droplets prepared using microfluidics as described in the experimental section. This experiment was repeated preparing the emulsions using a TissueLyser II (QIAGEN) without noticeable difference between the methods of emulsification (S5 Fig in S3 File).

AEGIS PCR with 6-letters

To demonstrate that droplets suspended in the iso-dense fluorinated oil had thermal stability adequate to support PCR and, in particular, PCR containing AEGIS bases, a double stranded DNA molecule with 49 bp containing the AEGIS pair Z:P (Fig 1) was used as template. The enzyme used to amplify this was a derivative of the *Taq* DNA polymerase where the amino acids 1–280 were deleted (removing the exonuclease domain), with the N-terminus of the catalytic domain fused to a processivity enhancing domain from *Sulfolobus solfataricus*. The *Taq* variant has 6 mutations, two specific for enhancing the incorporation of the pair **Z:P** (R587Q and E832G). The enzyme is described as: Sso7d-*Taq* (Δ 1–280) R587Q E626K I707L E708K A743H E832G.

Progress of the PCR was monitored by observing the fluorescence of Evagreen®, which intercalates into double-stranded PCR amplicons. Fig 12 shows real time PCR fluorescence signals arising from the PCR reaction. As a control a PCR done in bulk aqueous solution shows comparable fluorescence signals to the ones that come from water droplets emulsified in iso-dense fluorinated oil. These results showed that neither the surfactant nor the fluorinated oil had any measurable impact on the progress of the PCR. This is consistent with the orthogonality of the fluorinated oil and the surfactant with respect all biological molecules involved in the PCR.

Taqman® assay

One standard way to detect DNA is a Taqman® assay. Here, DNA polymerase from *Thermus aquaticus* degrades the downstream strand using its 5'-3' exonuclease activity displacing a probe from the template, cleaving the probe in the process. This cleavage separates a fluorescent reporter (here, fluorescein, FAM) from one end of the probe from a fluorescence quencher at the other end of the probe, to give a fluorescent signal.

Here, we adapted the Taqman® assay to detect a target analyte that contained AEGIS dZ and dP (Fig 1). As before, the aqueous phase was emulsified by mixing 100 μL of aqueous phase mixed with 300 μL of fluorinated oil (1 volume of LMW fraction and 4 volumes of the
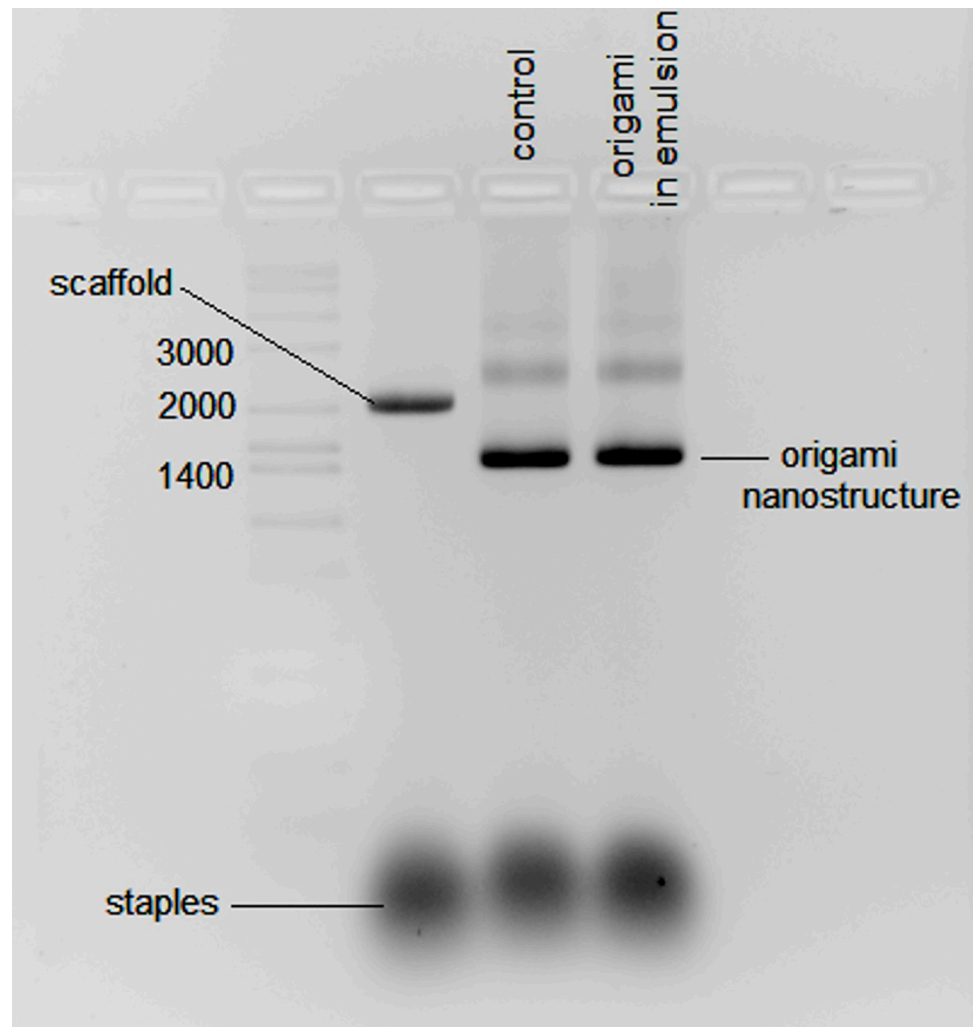
Fig 11. DNA electrophoresis in agarose (2%) showing the formation of origami structures in droplets. The origami products were run in 0.5 X Tris-borate EDTA buffer with ethidium bromide and 6 mM MgCl$_2$. The origami structure folded is called "nanostructure PF-2, cuboid with large aperture" from Tilibit Nanosystems. The scaffold, a single-stranded DNA type p7249 isolated from M13mp18 of length 7,249 bases. The staples are a mixture of 208 oligos (S1 Table in S3 File). A sample of the mixture of scaffold and staples not annealed is run for comparison. The origami folded properly shows a distinctive migration on the gel (see S8 and S9 Figs for reference in S3 File). Annealing was done by incubating at 65˚C for 10 minutes then cooled down from 60˚C to 40˚C at a rate of 1˚C per hour.

https://doi.org/10.1371/journal.pone.0252361.g011

HMW fraction, see protocol 1) with 2% of surfactant (a-R$_2$). Emulsions were made by shaking using a QIAGEN TissueLyser II (15 Hz for 10 seconds followed by 17 Hz for 7 seconds) in a Snap-Cap Microcentrifuge Biopur™ Safe-Lock™ tube containing a 6 mm stainless steel bead. Again, output was essentially the same as observed in bulk Taqman® assays (Fig 13). The *Taq* DNA polymerase variant used contains two mutations (R587Q, E832C) that favor the incorporation of the Z:P pair.

RCA in droplets

RCA works by having a circular template, a primer that binds to that circular template, and a strand displacing polymerase that extends that primer, displacing already synthesized DNA as it proceeds around the circle. Here, the aqueous phase used to prepare the droplets contains a
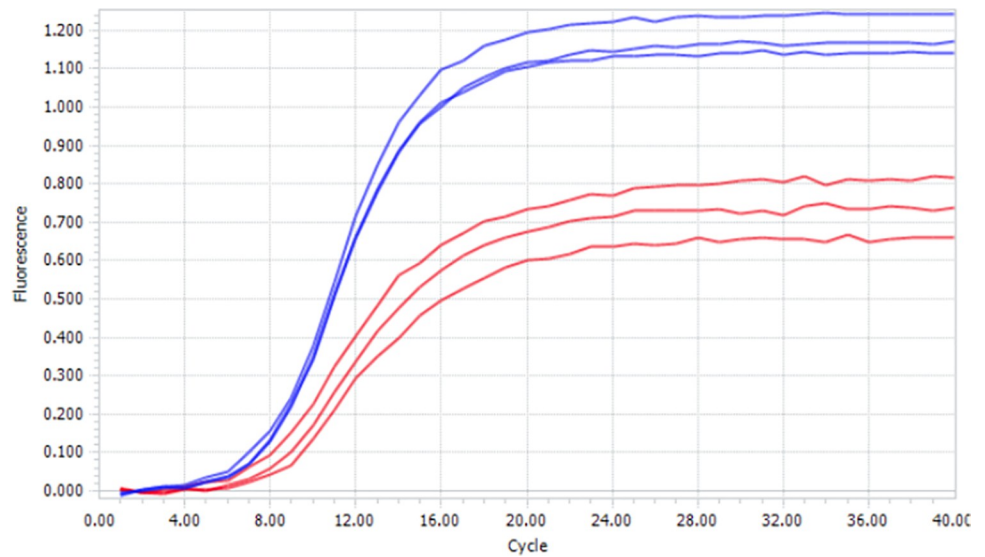
Fig 12. Real time PCR showing emergence of fluorescence from intercalated Evagreen® without emulsification (blue lines) and in the emulsified PCR (red lines). The aqueous phase was emulsified by mixing 100 μL of aqueous phase mixed with 300 μL of fluorinated oil (1 volume of LMW fraction and 4 volumes of the HMW fraction, see protocol 1) with 2% of surfactant (a-R₂). Assays done by triplicate.
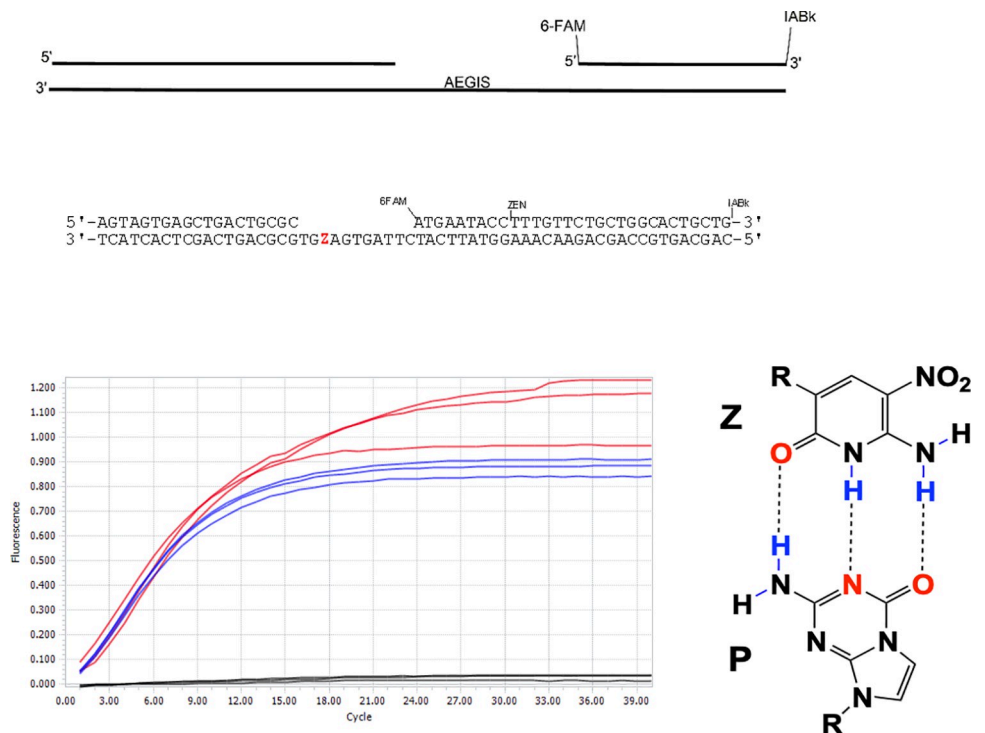
Fig 13. Taqman® assay in droplets. Top: Scheme of the Taqman® assay containing AEGIS (dZ:dP pair hydrogen bonding shown). Bottom: Real-time fluorescence detected from a probe. The probe contains a 5′ fluorophore: 6-carboxyfluorescein (6FAM) and is double-quenched with: 3′ Iowa Black™ (IABk) and a proprietary internal ZEN quencher (IDT). When *Taq* [R587Q E832C] polymerase places a dZ opposite dP and the 5'-3' exonuclease of *Taq* polymerase cleaves the probe eventually releasing a fluorescent molecule. The blue line is the fluorescence from a non-emulsified reaction. The red line corresponds to the signal from the emulsified reaction. The emulsion was made by mixing 100 μL of aqueous phase with 300 μL of a fluorinated oil with 2% (v/v) fluorinated surfactant as shown on Fig 2. Mixed in QIAGEN TissueLyser II in the presence of a 6 mm stainless steel bead at 15 Hz for 10 seconds followed by 17 Hz for 7 seconds using an Eppendorf Safe-Lock Tube (2 mL) containing a stainless steel ball. Assays were done by triplicate.
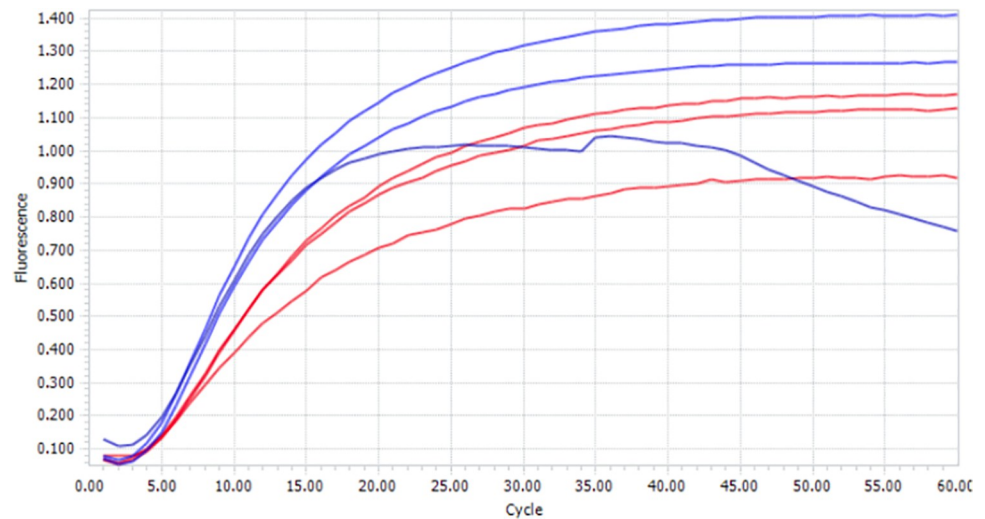
Fig 14. Amplification curves obtained using the LightCycler96 for RCA amplification in droplets. Fluorescence detection (EvaGreen®) is acquired after each two step cycle [37˚C for 30 seconds—37˚C for 30 seconds followed by aquisition] x 60 cycles. Blue lines correspond to the reaction that was not emulsified. Red lines correspond to the emulsified reaction. Assays done by triplicate.

https://doi.org/10.1371/journal.pone.0252361.g014

circularized template 96 nucleotides around, a primer complementary to the circular template, and dNTPs. The polymerase was Phi29 DNA polymerase. The progress of the RCA was followed by measuring fluorescence emitted by an intercalating fluorescent dye (EvaGreen®) in a Light Cycler over a period of 1 hour (Fig 14).

Discussion

The growing interest in synthetic cells [51] matches a growing interest in engineering enzymes for synthetic biology using directed evolution [52–54]. For example, Tawfik and Griffiths [26] developed a method to link genotype and phenotype in droplets of water emulsified in oil called "Compartmentalized Self-Replication" (CSR). This strategy was adapted in the Holliger laboratory for the directed evolution of DNA polymerases [10].

However, various laboratories have reported difficulties in reproducing CSR procedures. One of the first problems identified was associated to the surfactant Span 80® [55]. It is very likely that Span 80®, which is derived from animal fat, carries in uncontrolled amounts a problematic contaminant. Indeed, the Holliger group reports the need for an antioxidant to avoid oxidation due to peroxide contaminants in Span 80® [35]. Thus, while results are possible with surfactant mixtures containing Span 80®, these are hit-or-miss, and has become known in the community as problematically irreproducible.

For this reason, many have turned to synthetic materials and a third liquid phase, the "fluorous phase". Kobayashi and Owen reported some time ago the synthesis of non-ionic fluorosilicone surfactants with 3,3,3-trifluoropropyl and 3,3,4,4,5,5,6,6,6-nonafluorohexyl side chains with poly(oxyethylene) hydrophiles [50].

Here, balancing the mixture of hydrocarbon-carrying silanes, intrinsically less dense than water, with fluorohydrocarbon-carrying silanes, intrinsically more dense than water, yielded mixtures that had densities essentially identical to the density of water. As the density of water can change with different amounts of solutes, the density of the fluorinated oils described here can be changed by mixing the fractions, separated by distillation, in different ratios to match the desired density.

The fluorinated oils described here have been used to encapsulate different biochemical reactions such as DNA origami folding, PCR, Taqman® assay and RCA. We found no negative impact of the encapsulation. All of these biochemical reactions worked as well in these iso-dense fluorinated oil-surfactant systems as their non-emulsified analogs. Thus, they add a significant and important new resource for nanotechnology, directed evolution and synthetic biology.

Supporting information

S1 File. Molecular weight distribution raw data.
(JNB)

S2 File. Molecular weight distribution raw data.
(JNB)

S3 File. Supporting information. Additional figures and raw images.
(DOCX)

Acknowledgments

We thank Tamara Aigner and Jean-Philippe Sobczak from Tilibit Nanosystems for useful discussions and assistance in troubleshooting and confirming the formation of the origami nano-structure. We thank Brian Paegel laboratory for providing molds and assistance in preparing microfluidic devices as well as valuable discussions in surfactant design.

Author Contributions

Conceptualization: Roberto Laos, Steven Benner.

Data curation: Roberto Laos.

Investigation: Roberto Laos.

Writing – original draft: Roberto Laos.

Writing – review & editing: Roberto Laos, Steven Benner.

References

1. Paegel BM, Joyce GF. Microfluidic Compartmentalized Directed Evolution. Chemistry & Biology. 2010; 17(7):717–24. https://doi.org/10.1016/j.chembiol.2010.05.021 WOS:000280831100008. PMID: 20659684

2. Stucki A, Vallapurackal J, Ward TR, Dittrich PS. Droplet Microfluidics and Directed Evolution of Enzymes: An Intertwined Journey. Angewandte Chemie-International Edition. 2021: 21. https://doi.org/10.1002/anie.202016154 WOS:000673231300001. PMID: 33539653

3. Laos R, Shaw RW, Benner SA. Engineered DNA Polymerases. In: Murakami KS, Trakselis MA, editors. Nucleic Acid Polymerases. Nucleic Acids and Molecular Biology. 302014. p. 163–87.

4. Stucki A, Vallapurackal J, Ward TR, Dittrich PS. Droplet Microfluidics and Directed Evolution of Enzymes: An Intertwined Journey. Angewandte Chemie-International Edition. https://doi.org/10.1002/anie.202016154 WOS:000673231300001. PMID: 33539653

5. Buddingh BC, van Hest JCM. Artificial Cells: Synthetic Compartments with Life-like Functionality and Adaptivity. Accounts of Chemical Research. 2017; 50(4):769–77. https://doi.org/10.1021/acs.accounts.6b00512 WOS:000399859800013. PMID: 28094501

6. Elani Y. Interfacing Living and Synthetic Cells as an Emerging Frontier in Synthetic Biology. Angewandte Chemie International Edition. 2021; 60(11):5602–11. https://doi.org/10.1002/anie.202006941 PMID: 32909663

7. Akbarzadeh A, Rezaei-Sadabady R, Davaran S, Joo SW, Zarghami N, Hanifehpour Y, et al. Liposome: classification, preparation, and applications. Nanoscale Research Letters. 2013; 8. https://doi.org/10.1186/1556-276x-8-102 WOS:000316359300001. PMID: 23432972

8. Allen TM, Cullis PR. Liposomal drug delivery systems: From concept to clinical applications. Advanced Drug Delivery Reviews. 2013; 65(1):36–48. https://doi.org/10.1016/j.addr.2012.09.037 PMID: 230362257400008.

9. Lammers T, Kiessling F, Hennink WE, Storm G. Drug targeting to tumors: Principles, pitfalls and (pre-) clinical progress. Journal of Controlled Release. 2012; 161(2):175–87. https://doi.org/10.1016/j.jconrel.2011.09.063 WOS:000305790300004. PMID: 21945285

10. Ghadessy FJ, Ong JL, Holliger P. Directed evolution of polymerase function by compartmentalized self-replication. Proc Natl Acad Sci U S A. 2001; 98(8):4552–7. https://doi.org/10.1073/pnas.071052198 WOS:000168059700053. PMID: 11274352

11. Ghadessy FJ, Ramsay N, Boudsocq F, Loakes D, Brown A, Iwai S, et al. Generic expansion of the substrate spectrum of a DNA polymerase by directed evolution. Nature Biotechnology. 2004; 22(6):755–9. https://doi.org/10.1038/nbt974 WOS:000221785300038. PMID: 15156154

12. Laos R, Shaw R, Leal NA, Gaucher E, Benner S. Directed Evolution of Polymerases To Accept Nucleotides with Nonstandard Hydrogen Bond Patterns. Biochemistry. 2013; 52(31):5288–94. https://doi.org/10.1021/bi400558c WOS:000323013700017. PMID: 23815560

13. Laos R, Thomson JM, Benner SA. DNA Polymerases Engineered by Directed Evolution to Incorporate Nonstandard Nucleotides. Frontiers in Microbiology. 2014; 5. https://doi.org/10.3389/fmicb.2014.00565 PMID: 25400626

14. Yang JH, Tu R, Yuan HL, Wang QH, Zhu LL. Recent advances in droplet microfluidics for enzyme and cell factory engineering. Critical Reviews in Biotechnology. https://doi.org/10.1080/07388551.2021.1898326 WOS:000630753400001. PMID: 33730939

15. Kurihara K, Tamura M, Shohda K-i, Toyota T, Suzuki K, Sugawara T. Self-reproduction of supramolecular giant vesicles combined with the amplification of encapsulated DNA. Nat Chem. 2011; 3(10):775–81. https://doi.org/10.1038/nchem.1127 PMID: 219412497200010.

16. Luisi PL, Walde P, Oberholzer T. Lipid vesicles as possible intermediates in the origin of life. Current Opinion in Colloid & Interface Science. 1999; 4(1):33–9. https://doi.org/10.1016/s1359-0294(99)00012-6. WOS:000080941800005.

17. Stano P. Minimal cells: Relevance and interplay of physical and biochemical factors. Biotechnology Journal. 2011; 6(7):850–9. https://doi.org/10.1002/biot.201100079 WOS:000292738100009. PMID: 21648093

18. Walde P, Ichikawa S. Enzymes inside lipid vesicles: Preparation, reactivity and applications. Biomolecular Engineering. 2001; 18(4):143–77. https://doi.org/10.1016/s1389-0344(01)00088-0 WOS:000171578700001. PMID: 11576871

19. Caschera F, Noireaux V. Integration of biological parts toward the synthesis of a minimal cell. Current Opinion in Chemical Biology. 2014; 22:85–91. https://doi.org/10.1016/j.cbpa.2014.09.028 WOS:000345604000014. PMID: 25285755

20. Huang Y, Kim S-H, Arriaga LR. Emulsion templated vesicles with symmetric or asymmetric membranes. Advances in Colloid and Interface Science. 2017; 247:413–25. https://doi.org/10.1016/j.cis.2017.07.013 WOS:000412150100026. PMID: 28802479

21. Kamiya K, Takeuchi S. Giant liposome formation toward the synthesis of well-defined artificial cells. Journal of Materials Chemistry B. 2017; 5(30):5911–23. https://doi.org/10.1039/c7tb01322a WOS:000407083800001. PMID: 32264347

22. Matosevic S. Synthesizing artificial cells from giant unilamellar vesicles: State-of-the art in the development of microfluidic technology. Bioessays. 2012; 34(11):992–1001. https://doi.org/10.1002/bies.201200105 WOS:000309910400015. PMID: 22926929

23. Supramaniam P, Ces O, Salehi-Reyhani A. Microfluidics for Artificial Life: Techniques for Bottom-Up Synthetic Biology. Micromachines. 2019; 10(5). https://doi.org/10.3390/mi10050299 WOS:000470966700022. PMID: 31052344

24. Trantidou T, Friddin MS, Salehi-Reyhani A, Ces O, Elani Y. Droplet microfluidics for the construction of compartmentalised model membranes. Lab on a Chip. 2018; 18(17):2488–509. https://doi.org/10.1039/c8lc00028j WOS:000443279400001. PMID: 30066008

25. van Swaay D, deMello A. Microfluidic methods for forming liposomes. Lab on a Chip. 2013; 13(5):752–67. https://doi.org/10.1039/c2lc41121k WOS:000314651000001. PMID: 23291662

26. Tawfik DS, Griffiths AD. Man-made cell-like compartments for molecular evolution. Nature Biotechnology. 1998; 16(7):652–6. https://doi.org/10.1038/nbt0798-652 WOS:000074521800029. PMID: 9661199

27. Singh I, Laos R, Hoshika S, Benner SA, Georgiadis MM. Snapshots of an evolved DNA polymerase pre- and post-incorporation of an unnatural nucleotide. Nucleic Acids Research. 2018; 46(15):7977–88. https://doi.org/10.1093/nar/gky552 WOS:000444148100043. PMID: 29986111

28. Benner SA, Karalkar NB, Hoshika S, Laos R, Shaw RW, Matsuura M, et al. Alternative Watson-Crick Synthetic Genetic Systems. Cold Spring Harbor Perspectives in Biology. 2016; 8(11):26. https://doi.org/10.1101/cshperspect.a023770 WOS:000389841300005. PMID: 27663774

29. Zhang LQ, Yang ZY, Trinh TL, Teng IT, Wang S, Bradley KM, et al. Aptamers against Cells Overexpressing Glypican 3 from Expanded Genetic Systems Combined with Cell Engineering and Laboratory Evolution. Angewandte Chemie-International Edition. 2016; 55(40):12372–5. https://doi.org/10.1002/anie.201605058 WOS:000384713700041. PMID: 27601357

30. Biondi E, Lane JD, Das D, Dasgupta S, Piccirilli JA, Hoshika S, et al. Laboratory evolution of artificially expanded DNA gives redesignable aptamers that target the toxic form of anthrax protective antigen. Nucleic Acids Research. 2016; 44(20):9565–77. https://doi.org/10.1093/nar/gkw890 WOS:000393817800011. PMID: 27701076

31. Duffy K, Arangundy-Franklin S, Holliger P. Modified nucleic acids: replication, evolution, and next-generation therapeutics. Bmc Biology. 2020; 18(1). https://doi.org/10.1186/s12915-020-00803-6 WOS:000568198200001. PMID: 32878624

32. Jena NR, Pant S, Srivastava HK. Artificially expanded genetic information systems (AEGISs) as potent inhibitors of the RNA-dependent RNA polymerase of the SARS-CoV-2. Journal of Biomolecular Structure & Dynamics. 2021: 17. https://doi.org/10.1080/07391102.2021.1883112 WOS:000616859200001. PMID: 33565387

33. Baret JC. Surfactants in droplet-based microfluidics. Lab on a Chip. 2012; 12(3):422–33. https://doi.org/10.1039/c1lc20582j WOS:000298964300003. PMID: 22011791

34. Dai B, Leal LG. The mechanism of surfactant effects on drop coalescence. Physics of Fluids. 2008;20 (4). https://doi.org/10.1063/1.2911700 WOS:000255456600012.

35. Ramsay N, Jemth A-S, Brown A, Crampton N, Dear P, Holliger P. CyDNA: Synthesis and Replication of Highly Cy-Dye Substituted DNA by an Evolved Polymerase. Journal of the American Chemical Society. 2010; 132(14):5096–104. https://doi.org/10.1021/ja909180c WOS:000276553700036. PMID: 20235594

36. Ghadessy FJ, Holliger P. A novel emulsion mixture for in vitro compartmentalization of transcription and translation in the rabbit reticulocyte system. Protein Engineering Design & Selection. 2004; 17(3):201–4. https://doi.org/10.1093/protein/gzh025 WOS:000222797300001. PMID: 14990785

37. Diehl F, Li M, He YP, Kinzler KW, Vogelstein B, Dressman D. BEAMing: single-molecule PCR on microparticles in water-in-oil emulsions. Nature Methods. 2006; 3(7):551–9. https://doi.org/10.1038/nmeth898 WOS:000238669600018. PMID: 16791214

38. Chiu YL, Chan HF, Phua KKL, Zhang Y, Juul S, Knudsen BR, et al. Synthesis of Fluorosurfactants for Emulsion-Based Biological Applications. Acs Nano. 2014; 8(4):3913–20. https://doi.org/10.1021/nn500810n WOS:000334990600089. PMID: 24646088

39. Riess JG. Fluorous micro- and nanophases with a biomedical perspective. Tetrahedron. 2002; 58 (20):4113–31. https://doi.org/10.1016/s0040-4020(02)00262-4 WOS:000175612700037.

40. Riess JG. Fluorocarbon-based injectable gaseous microbubbles for diagnosis and therapy. Current Opinion in Colloid & Interface Science. 2003; 8(3):259–66. https://doi.org/10.1016/s1359-0294(03)00047-5 WOS:000184757000008.

41. Riess JG. Fluorocarbon-based oxygen-delivery: Basic principles and product development. Blood Substitutes: Principles, Methods, Products and Clinical Trials, Vol 2. 1998:101–26. CCC:000072284300006.

42. Riess JG. Oxygen carriers ("blood substitutes")—Raison d'Etre, chemistry, and some physiology. Chemical Reviews. 2001; 101(9):2797–919. https://doi.org/10.1021/cr970143c WOS:000171047000007. PMID: 11749396

43. Schutt EG, Klein DH, Mattrey RM, Riess JG. Injectable microbubbles as contrast agents for diagnostic ultrasound imaging: The key role of perfluorochemicals. Angewandte Chemie-International Edition. 2003; 42(28):3218–35. https://doi.org/10.1002/anie.200200550 WOS:000184465000003. PMID: 12876730

44. Abate AR, Weitz DA. High-Order Multiple Emulsions Formed in Poly(dimethylsiloxane) Microfluidics. Small. 2009; 5(18):2030–2. https://doi.org/10.1002/smll.200900569 WOS:000270342500001. PMID: 19554565

45. Mazutis L, Araghi AF, Miller OJ, Baret JC, Frenz L, Janoshazi A, et al. Droplet-Based Microfluidic Systems for High-Throughput Single DNA Molecule Isothermal Amplification and Analysis. Analytical Chemistry. 2009; 81(12):4813–21. https://doi.org/10.1021/ac900403z WOS:000266969700019. PMID: 19518143

46. Fidalgo LM, Abell C, Huck WTS. Surface-induced droplet fusion in microfluidic devices. Lab on a Chip. 2007; 7(8):984–6. https://doi.org/10.1039/b708091c WOS:000248281600013. PMID: 17653339

47. Marcoux PR, Dupoy M, Mathey R, Novelli-Rousseau A, Heran V, Morales S, et al. Micro-confinement of bacteria into w/o emulsion droplets for rapid detection and enumeration. Colloids and Surfaces a-Physicochemical and Engineering Aspects. 2011; 377(1–3):54–62. https://doi.org/10.1016/j.colsurfa.2010.12.013 WOS:000288773900007.

48. Schonbrun E, Abate AR, Steinvurzel PE, Weitz DA, Crozier KB. High-throughput fluorescence detection using an integrated zone-plate array. Lab on a Chip. 2010; 10(7):852–6. https://doi.org/10.1039/b923554j WOS:000275757600010. PMID: 20300671

49. Yactine B, Ratsimihety A, Ganachaud F. Do-it-yourself functionalized silicones part 2: synthesis by ring opening polymerization of commercial cyclosiloxanes. Polymers for Advanced Technologies. 2010; 21 (2):139–49. https://doi.org/10.1002/pat.1509 WOS:000274173200008.

50. Kobayashi H, Owen MJ. Nonionic Fluorosilicone Surfactants. Journal of Colloid and Interface Science. 1993; 156(2):415–9. https://doi.org/10.1006/jcis.1993.1131 WOS:A1993KT88300023.

51. Nie P, Bai Y, Hui M. Synthetic Life with Alternative Nucleic Acids as Genetic Materials. Molecules. 2020; 25(15):3483. https://doi.org/10.3390/molecules25153483 PMID: 32751873

52. Nikoomanzar A, Chim N, Yik EJ, Chaput JC. Engineering polymerases for applications in synthetic biology. Quarterly Reviews of Biophysics. 2020;53. https://doi.org/10.1017/S0033583520000050 WOS:000552696100001. PMID: 32715992

53. Ouaray Z, Singh I, Georgiadis MM, Richards NGJ. Building better enzymes: Molecular basis of improved non-natural nucleobase incorporation by an evolved DNA polymerase. Protein Science. 2020; 29(2):455–68. https://doi.org/10.1002/pro.3762 WOS:000496314100001. PMID: 31654473

54. Coulther TA, Stern HR, Beuning PJ. Engineering Polymerases for New Functions. Trends in Biotechnology. 2019; 37(10):1091–103. https://doi.org/10.1016/j.tibtech.2019.03.011 WOS:000485189600009. PMID: 31003719

55. R. L. Directed evolution of polymerases to accept nucleotides with non-strandard hydrogen bonding patterns. Florida, USA: University of Florida; 2015.